Published in final edited form as:

Neuroradiology. 2018 August ; 60(8): 795–802. doi:10.1007/s00234-018-2041-1.

Quantitative Sodium Imaging and Gliomas: A Feasibility Study

Lucidio P. Nunes Neto, MD[1], **Guillaume Madelin, PhD**[1], **Terlika Sood**[1], **Chih-Chin Wu, MD**[1], **Douglas Kondziolka, MD**[2], **Dimitris Placantonakis, MD, PhD**[2], **John G. Golfinos, MD**[2], **Andrew Chi, MD, PhD**[3], and **Rajan Jain, MD**[1,2,*]

[1]Department of Radiology, New York University School of Medicine New York, NY USA

[2]Department of Neurosurgery, New York University School of Medicine New York, NY USA

[3]Department of Medicine, New York University School of Medicine New York, NY USA

Abstract

Purpose: Recent advances in sodium brain MRI have allowed for increased signal-to-noise ratio, faster imaging and the ability of differentiating intracellular from extracellular sodium concentration, opening a new window of opportunity for clinical application. In gliomas there are significant alterations in sodium metabolism, including increase in total sodium concentration and extracellular volume fraction. The purpose of this study is to assess the feasibility of using sodium MRI quantitative measurements to evaluate gliomas.

Methods: Eight patients with treatment naïve gliomas were scanned at 3 Tesla with a homemade $^{1}H/^{23}Na$ head coil, generating maps of pseudo-intracellular sodium concentration (C_1), pseudo-extracellular volume fraction (α_2), apparent intracellular sodium concentration (aISC) and apparent total sodium concentration (aTSC). Measurements were made within the contralateral normal appearing putamen, contralateral normal appearing white matter (NAWM) and in solid tumor regions (area of T2-FLAIR abnormality, excluding highly likely areas of edema, cysts, or necrosis). Paired samples t-test were performed comparing NAWM and putamen and between NAWM and solid tumor.

Results: Normal appearing putamen demonstrated significantly higher values for aTSC, aISC, C_1 ($p<0.001$), and α_2 ($p=0.002$) when compared to NAWM. Mean average of all solid tumors, when compared to NAWM, demonstrated significantly higher values of aTSC and α_2 ($p<0.001$), and significantly lower values of aISC ($p=0.02$), There was no significant difference between the values of C_1 ($p=0.19$).

Conclusion: Quantitative sodium measurements can be done in glioma patients and also has provided further evidence that total sodium and extracellular volume fraction are increased in gliomas.

Corresponding Author's name and complete mailing address: Rajan Jain, MD, Associate Professor, Radiology and Neurosurgery, NYU School of Medicine, 660 First Avenue, 2nd Floor, New York, NY 10016, Phone: 212-263-5219, Fax: 212-263-3838, rajan.jain@nyumc.org.

Note: Oral presentation at the American Society of Neuroradiology (ASNR) 55th Annual Meeting, April 24–27, 2017 at the Long Beach, California.

Keywords

Sodium; MRI; Glioma

Introduction

Sodium (^{23}Na) plays a major role in normal cell metabolism, with a gradient of concentration between the intracellular and extracellular compartments being responsible for generating resting membrane potential, transmitting nerve impulses and contributing to the uptake of the neurotransmitter glutamate[1]. Sodium is also closely related to apoptosis, either in a normal or pathological state, with changes in ion homeostasis being an early and key stage[2].

Sodium brain magnetic resonance imaging (MRI) has been studied for over 30 years, with data demonstrating the ability to correlate voxel intensity to sodium concentration[3]. However, several limitations, including significantly lower signal-to-noise ratio (SNR) compared to proton MRI, due to smaller sodium concentration and nuclear magnetic resonance (NMR) receptivity, prevented the development of clinical applications[4]. Another major obstacle for the earlier studies involved the inability to make a clear distinction between intracellular and extracellular sodium concentration; which make it difficult to differentiate alterations due to increase in the extracellular volume fraction (at constant sodium concentration around 140 mM), such as vasogenic edema, from alterations due to increase of intracellular sodium (from equilibrium sodium concentration of around 10–20 mM in normal brain tissue), such as neoplasm with high proliferation rates[5].

Recently, the development of MRI scanners with higher magnetic fields (≥3 T) enabled increased SNR, and the development of new ways of acquiring data, like fast three-dimensional acquisition allowed faster imaging[6–8]. Moreover, techniques to determine intracellular sodium concentration were also developed, opening a new window of opportunity for clinical application[7, 9]. Considerable knowledge has also been gained regarding in vivo ^{23}Na T_1 and T_2 biexponential relaxation, caused by interactions between the sodium cations and macromolecular electric field gradients in their surroundings. A recent study demonstrated with a biexponential relaxation model that white matter, gray matter and the subcortical regions present differences between the signal contributions of short and long components of T_2 relaxation. This must be taken into consideration when trying to quantify sodium measures with MRI signal[10].

In tumors, there are significant alterations in sodium metabolism, with an increase in intracellular sodium being more pronounced in rapidly dividing cells[11]. Also, the ability to retain higher intracellular concentrations of sodium and other ions could be key for a tumor cell to avoid apoptosis[12]. It is thus possible that sodium MRI could add valuable information about tumor growth rate and response to treatment, contributing to better management of brain tumor patients.

The purpose of this pilot study is to measure pseudo-intracellular sodium concentration (C_1), extracellular volume fraction (α_2), apparent intracellular sodium concentration (aISC) and

apparent total sodium concentration (aTSC) in patients with treatment naïve gliomas using sodium MR imaging.

Materials and Methods/Case Material

Ethics Statement

This study was approved by the institutional review board (IRB) and performed in compliance with the Health Insurance Portability and Accountability Act (HIPAA). All subjects provided written informed consent.

Patient Cohort

The inclusion criteria were patients with a suspected diagnosis of a glioma, over 18 years old, and treatment naïve. The final number of patients enrolled was 8: six World Health Organization (WHO) grade II, one grade III, and one grade IV.

MR Imaging

Patients were scanned at 3 Tesla (PRISMA system, Siemens, Erlangen, Germany) with an 8-channel transmit-receive dual-tuned $^{1}H/^{23}Na$ head coil (homemade). Two ^{23}Na MRI were performed: (1) FLORET: 3 hubs, cone angle 45°, 120 interleaves/hub, FA 80°/1 ms, TE 0.2 ms, TR 100 ms, FOV 320 mm, resolution 5 mm isotropic, 20 averages, TA 12:00 min; (2) FLORET with fluid suppression by inversion recovery (IR): same parameters as (1) except: inversion pulse 180°/6 ms, TI 25 ms, FA 90°/1 ms, 30 averages, TA 18:00 min.[12,19] Images were reconstructed offline in Matlab (Mathworks, Natick, MA, USA) with 3D regridding and nominal isotropic resolution of 2.5 mm. Two ^{1}H MRI were also performed: (1) 3D FLAIR: 1.25 mm isotropic resolution, FOV 320 mm, TR 6000 ms, TI 21000 ms, TE 351 ms, echo train length 240, TA 4:36 min; (2) 3D MPRAGE: 1.25 mm isotropic resolution, FOV 320 mm, TR 2100 ms, TI 900 ms, TE 4.27 ms, TA 4:17 min. Average overall time of acquisition for all ^{1}H and ^{23}Na data was 45–50 min (including shimming and localizer), during which the patient stayed in the scanner (no change of coil was necessary) and asked to not move during the whole exam (cushions were also placed on each side of the head to stabilize it and reduce possibilities of movement). All proton (3D MPRAGE and 3D FLAIR) and sodium (3D FLORET) images were acquired centered at the isocenter of the system with the same RF coil, and were therefore naturally co-registered (same center, same FOV). Upon visual comparison of the ^{1}H and ^{23}Na images, if there was any doubt that the patient moved during one scan, images were co-registered again using SPM12 (http://www.fil.ion.ucl.ac.uk/spm/software/spm12/). Only for one subject (patient no. 5) did we have to realign the sodium images acquired with IR, as the patient managed to rotate his head between the two sodium acquisitions. As a measure of precaution, alignment of all proton and sodium images was subsequently verified in SPM12 for each subject, with the MPRAGE image as a reference: no variation (rotation or translation of the head) was detectable with the algorithm (the resulting rotation matrix was unity in all cases), and therefore no further coregistration was necessary.

Sodium data quantifcation

Both ^{23}Na acquisitions were used to generate C_1, α_2, aTSC, and aISC maps of whole brain using linear regression of gel reference phantom as described below[7, 13]. C_1 and α_2 quantification was based on a simple three-compartment model shown in Figure 1. In this model, the extracellular compartment has a constant sodium concentration of 140 mM (C_2), water volume fraction is considered constant at w = 0.775 in this preliminary study (average of water fraction in white and gray matters), and extracellular fluid sodium signals are considered mostly suppressed (or attenuated within noise level) by inversion recovery. We will use the notation S_1 = aTSC and S_2 = aISC in the following equations. With these assumptions, $C_1 = C_2S_2 / (C_2w – S_2 + S_1)$ and $\alpha_2 = (S_1 – S_2)/C_2$. The quantification process is as follows: (1) acquisition with and without fluid suppression by IR; (2) linear regression from the ^{23}Na signal of calibration phantoms; calculation of aTSC and aISC maps from the linear regression; (3) calculation of C_1 and α_2 maps based on the three-compartment model, with $C_1 = C_2S_2 / (C_2w – S_2 + S_1)$ and $\alpha_2 = (S_1 – S_2)/C_2$. For a more extensive explanation please see Madelin et al., 2014.[12] It can be noticed that the pairs of measurements C_1-α_2 and aTSC-aISC should carry the same information about the tissue: C_1 and α_2 were calculated from aTSC and aISC included in a simple three-compartment model of the brain tissue, in order to try to assess more physiologically relevant and more specific values related to intracellular sodium concentration and extracellular volume fraction (or cell density). The terms ‘apparent’ and ‘pseudo’ in the denominations of these measures were also included in order to take into account uncertainties in their calculations due to different parameters such as low signal-to-noise ratio of sodium MRI, imperfect inversion pulses leading to incomplete fluid suppression, variable relaxation times between subjects, and a simplistic three-compartment model.

Image Processing

All measurements on the co-registered ^{23}Na images and ^{1}H images were performed offline using the software ImageJ (National Institutes of Health, Bethesda, MD, USA). A circular region of interest (ROI) with a 52 mm^2 area was positioned in the contralateral normal appearing putamen on the ^{1}H image (FLAIR or MPRAGE) for measurements of C_1, α_2, aTSC, and aISC. Three similar ROIs were positioned in the normal appearing contralateral white matter. Free drawn ROIs were utilized to perform the same measurements in solid tumor regions (areas of T2-FLAIR abnormality, excluding highly likely areas of edema, cysts, or necrosis, according to ^{1}H MRI interpretation).

Statistical Analysis

Statistical analysis was performed by using paired samples t-test comparing values of C_1, α_2, aTSC, and aISC between normal appearing white matter (NAWM) and normal appearing putamen and between NAWM and areas of solid tumor.

Results

Among the eight patients, analysis of the NAWM revealed mean aTSC values of 30.30 ± 3.53 mM, mean α_2 of 17.17 ± 2.31 %, mean aISC of 6.23 ±1.83 mM, and mean C_1 of 10.47 ± 3.05 mM. Regarding the putamen, mean values of aTSC were 34.95 ± 4.16 mM,

mean values of α_2 were 18.89 ± 2.80 %, mean values of aISC were 8.49 ± 2.65 mM, and mean values of C_1 were 14.65 ± 4.40 mM. Analysis of the solid components of all eight tumors revealed mean aTSC values of 59.21 ±11.19 mM, mean α_2 values of 39.35 ± 8.21 %, mean aISC values of 4.33 ± 2.17 mM, and mean C_1 values of 12.2 ± 5.89 mM. The diagnoses and quantitative sodium measurements for the eight patients are summarized in Table 1.

Figure 2 shows the measurements of aTSC, aISC, C_1 and α_2 in ROIs in solid tumor and in normal appearing white matter all patients. Comparison between NAWM and solid components of the tumors performed by paired samples t-test revealed mean average of all solid tumors, when compared to NAWM, demonstrated significantly higher values of aTSC and α_2 ($p<0.001$), and significantly lower values of aISC ($p=0.02$), There was no significant difference between the values of C_1 ($p=0.19$) (Fig. 2).

To illustrate these findings we present two cases. First, a patient with diffuse astrocytoma, WHO grade II, IDH-mutated, without 1p/19 codeletion, where sodium imaging demonstrates in the solid tumor increased values of aTSC and α_2, and decreased values of aISC and C_1, in comparison to the contralateral NAWM (Fig. 3). The second case is a patient with an IDH-wildtype glioblastoma, WHO grade IV, where in proton imaging it is demonstrated a central necrotic area and a contrast-enhancing solid component. Sodium imaging demonstrates in the solid tumor increased values of aTSC and α_2, and values of aISC and C_1 similar to NAWM (Fig 4.). Figure 3 and 4 both show representative proton image and aTSC, aISC, C_1 and α_2 maps and ROI measurements in the patients. Note the difference in scaling in the C_1 maps in Figures 3E (0–20 mM) and 4E (0–90 mM), which were chosen such that these maps show the best contrast between the tumor and NAWM in each case.

Discussion

In normal brain tissue, the intracellular sodium concentration is within the range of 10–20 mM and the extracellular volume fraction is around 20%, resulting in a total sodium concentration than ranges from 36 to 42 mM[4, 7]. In our study, the values of C_1 and α_2 for normal appearing white matter and putamen were within this range, with somewhat lower values of aTSC than previously reported.

Our results showed higher values of aTSC in the putamen than in the white matter, in discordance to what was demonstrated by Ridley et al [10]. This might be explained by the fact that our white matter analysis was based on three ROIs, one of them in the centrum semiovale, a location where they also found lower values of total sodium concentration,

The solid component of tumors demonstrated higher values of aTSC than the white matter in all cases. This is in accordance with two other publications that analyzed the relation between total sodium concentration and gliomas, and could be explained by either an increase in intracellular concentration, increase in the extracellular volume fraction, or a combination of both[14, 15]. Another article demonstrated increased total sodium signal in 15 of the 16 brain tumors analyzed, including WHO grades I to IV and metastases[16].

Increases in total sodium concentration can also be related to other pathological states, and in this context it is important to highlight recent evidence demonstrating chronic elevation in epileptic patients, even during the interictal state[17]. Patients with gliomas can develop epilepsy and we did not exclude patients that presented seizures, so this could be a confounding factor and contribute to the raise in total sodium concentration demonstrated.

All our cases also demonstrated higher values of α_2 in the solid tumor component than in the normal appearing white matter, this being the major factor responsible for the increase in aTSC. An increase in the extracellular volume fraction in tumors has been reported previously, and attributed mainly to breakdown of the blood-brain barrier, edema, cysts, or necrosis[16]. However, our results demonstrate that it also occurs within the solid components of tumors. This finding could be related to, among other factors, differences in cell packing, loss of gap junctions between glioma cells, and migration of ions from the intracellular compartment, leading to cell shrinkage[14, 18]. Several studies, utilizing different experimental methods to access the extracellular space, confirmed the increase in its volume in both low-grade and high-grade gliomas, and even suggested a positive relation between the ability of a tumor in inducing enlargement of the intercellular space and its degree of aggressive behavior[18–22].

Analysis of all tumors as a group revealed lower levels of aISC than in the normal appearing white matter. Previous articles demonstrated increased intracellular sodium in high grade gliomas, and positive correlations between intracellular sodium and both MIB-1 proliferation rate and Ki-67 proliferation index, attributing this results to higher proliferation rates generating energetic breakdown of the Na^+/K^+-ATPase and sustained cell depolarization initiating cell division[16, 23]. Considering that seven of the eight tumors from our analysis are grades WHO II or III, it was not unexpected that many demonstrated low aISC. In fact, glioblastoma was the only tumor in our analysis to demonstrate higher aISC than the contralateral normal appearing white matter.

In recent years, greater relevance has been attributed to the role of sodium metabolism in the natural history of gliomas. Upregulation of the Na^+/H^+ exchanger isoform 1 (NHE1), leading to increased intracellular sodium and increased intracellular pH, has been implicated in promoting glioma proliferation, invasion and resistance to temozolomide therapy[24, 25]. Another study demonstrated that in oligodendrogliomas, IDH-mutated and 1p/19q codeleted, the NHE1 on 1p is silenced, and proposes that this could be a major contributor to the low proliferation rates in these tumors[26]. As the evidence of differences in sodium metabolism among gliomas grows, sodium MRI could increase its role in the characterization and management of these tumors.

Our pilot study has limitations, mainly the small number of patients and specially the small numbers of glioblastomas, preventing comparisons between high grade and low grade tumors as well as between IDH-mutated and IDH-wildtype gliomas. The long scan time is still a major obstacle for regular clinical use, and also facilitates the appearance of motions artifacts, degrading image quality and limiting coregistration accuracy. Another limitation regards the necessity of the model to assume that water fraction is constant, although differences between gray and white matter and between different subregions of the brain

have been demonstrated[27–29]. This permits only the determination of apparent total and intracellular sodium concentrations and pseudo-intracellular sodium concentration. Our model also does not considers the differences between the signal contributions of short and long components of T_2 relaxation present in subdivisions of the brain[10]. Similar to a limitation faced by dynamic susceptibility contrast (DSC) MR perfusion, comparing normal appearing white matter with gliomas can be misleading, as the tumor may be originated from a region with different normal sodium concentrations than white matter, and awareness is necessary.

Conclusion

The study demonstrates that quantitative sodium measurements can be done in glioma patients and also has provided further evidence that total sodium and extracellular volume fraction are increased in gliomas, though findings need to be validated by larger studies. Future studies could also provide valuable information about the utility of intracellular sodium measurements in distinguishing tumors with different genomic expression.

References

1. Ouwerkerk R (2011) Sodium MRI In: Modo M and Bulte J Magnetic Resonance Neuroimaging, Humana Press, New York, pp 175–201
2. Maeno E , Takahashi N , and Okada Y (2006) Dysfunction of regulatory volume increase is a key component of apoptosis. FEBS Lett 580:6513–651717101138
3. Perman W , Turski P , Houston L , (1986) Methodology of in vivo human sodium MR imaging at 1.5 T. Radiology 160:811–8203737922
4. Madelin G and Regatte R (2013) Biomedical applications of sodium MRI in vivo. J Magn Reson Imaging 38:511–52923722972
5. Turski P , Houston L , Perman W , (1987) Experimental and human brain neoplasms: detection with in vivo sodium MR imaging. Radiology 163:245–2493029803
6. Boada F , Gillen J , Shen G , (1997) Fast three dimensional sodium imaging. Magn Reson Med 37:706–7159126944
7. Madelin G , Kline R , Walvick R , (2014) A method for estimating intracellular sodium concentration and extracellular volume fraction in brain in vivo using sodium magnetic resonance imaging. Sci Rep 4:476324755879
8. Pipe J , Zwart N , Aboussouan E , (2011) A new design and rationale for 3D orthogonally oversampled k-space trajectories. Magn Reson Med 66:1303–131121469190
9. Boada F , Tanase C , Davis D , (2004) Non-invasive assessment of tumor proliferation using triple quantum filtered 23/Na MRI: technical challenges and solutions. Conf Proc IEEE Eng Med Biol Soc 7:5238–524117271521
10. Ridley B , Nagel AM , Bydder M , (2018) Distribution of brain sodium long and short relaxation times and concentrations: a multi-echo ultra-high field (23)Na MRI study. Sci Rep 8:435729531255
11. Cameron I , Smith N , Pool T , (1980) Intracellular concentration of sodium and other elements as related to mitogenesis and oncogenesis in vivo. Cancer Res 40:1439–14500
12. Cong D , Zhu W , Kuo J , (2015) Ion transporters in brain tumors. Curr Med Chem 22:1171–118125620102
13. Madelin G , Babb J , Xia D , (2015) Repeatability of quantitative sodium magnetic resonance imaging for estimating pseudo-intracellular sodium concentration and pseudo-extracellular volume fraction in brain at 3 T. PLoS One 10:e011869225751272
14. Bartha R , Megyesi J , and Watling C (2008) Low-grade glioma: correlation of short echo time 1H-MR spectroscopy with 23Na MR imaging. AJNR Am J Neuroradiol 29:464–47018238848

15. Ouwerkerk R , Bleich K , Gillen J , (2003) Tissue sodium concentration in human brain tumors as measured with 23Na MR imaging. Radiology 227:529–53712663825
16. Nagel A , Bock M , Hartmann C , (2011) The potential of relaxation-weighted sodium magnetic resonance imaging as demonstrated on brain tumors. Invest Radiol 46:539–54721577129
17. Ridley B , Marchi A , Wirsich J , (2017) Brain sodium MRI in human epilepsy: Disturbances of ionic homeostasis reflect the organization of pathological regions. Neuroimage 157:173–18328602596
18. Zamecnik J , Vargova L , Homola A , (2004) Extracellular matrix glycoproteins and diffusion barriers in human astrocytic tumours. Neuropathol Appl Neurobiol 30:338–35015305979
19. Zamecnik J (2005) The extracellular space and matrix of gliomas. Acta Neuropathol 110:435–44216175354
20. Bakay L (1970) The extracellular space in brain tumours. I. Morphological considerations. Brain 93:693–6984321422
21. Bakay L (1970) The extracellular space in brain tumours. II. The sucrose space. Brain 93:699–7084321423
22. Vargova L , Homola A , Zamecnik J , (2003) Diffusion parameters of the extracellular space in human gliomas. Glia 42:77–8812594739
23. Biller A , Badde S , Nagel A , (2016) Improved Brain Tumor Classification by Sodium MR Imaging: Prediction of IDH Mutation Status and Tumor Progression. AJNR Am J Neuroradiol 37:66–7326494691
24. Cong D , Zhu W , Shi Y , (2014) Upregulation of NHE1 protein expression enables glioblastoma cells to escape TMZ-mediated toxicity via increased H(+) extrusion, cell migration and survival. Carcinogenesis 35:2014–202424717311
25. Zhu W , Carney K , Pigott V , (2016) Glioma-mediated microglial activation promotes glioma proliferation and migration: roles of Na+/H+ exchanger isoform 1. Carcinogenesis 37:839–85127287871
26. Blough M , Al-Najjar M , Chesnelong C , (2012) DNA hypermethylation and 1p Loss silence NHE-1 in oligodendroglioma. Ann Neurol 71:845–84922718548
27. Koessler L , Colnat-Coulbois S , Cecchin T , (2017) In-vivo measurements of human brain tissue conductivity using focal electrical current injection through intracerebral multicontact electrodes. Hum Brain Mapp 38:974–98627726249
28. Gelman N , Ewing JR , Gorell JM , (2001) Interregional variation of longitudinal relaxation rates in human brain at 3.0 T: relation to estimated iron and water contents. Magn Reson Med 45:71–7911146488
29. Krebs N , Langkammer C , Goessler W , (2014) Assessment of trace elements in human brain using inductively coupled plasma mass spectrometry. J Trace Elem Med Biol 28:1–724188895

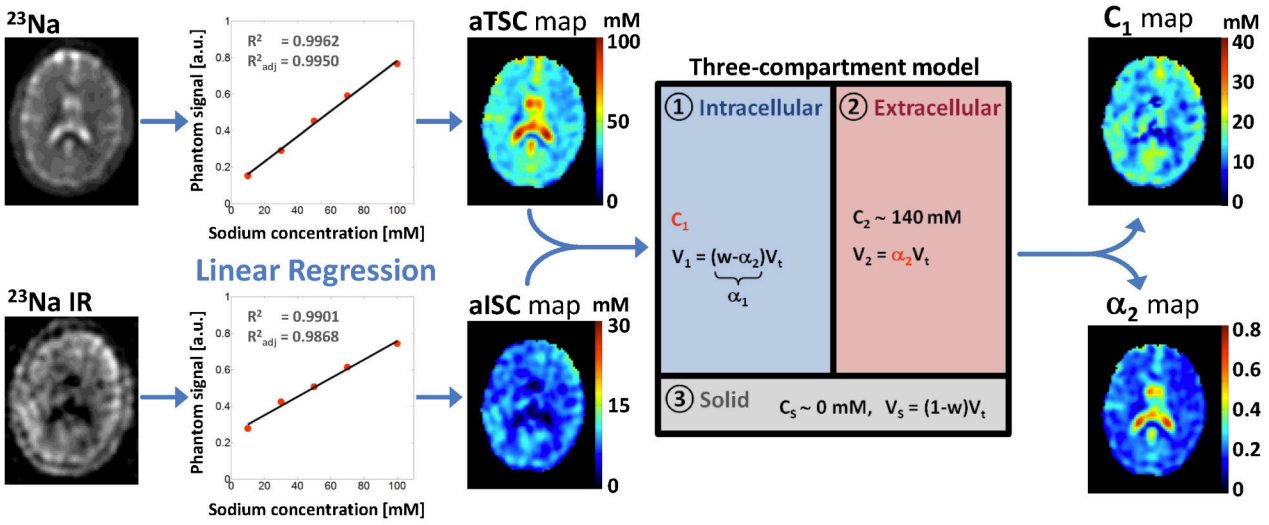

Fig. 1.

Diagram of the brain ^{23}Na MRI data processing steps: (1) acquisition with and without fluid suppression by IR; (2) linear regression from the ^{23}Na signal of calibration phantoms; calculation of aTSC and aISC maps from the linear regression; (3) calculation of C_1 and α_2 maps based on the three-compartment model, with $C_1 = C_2S_2 / (C_2w – S_2 + S_1)$ and $\alpha_2 = (S_1 – S_2)/C_2$. In this model C_2 = 140 mM (extracellular compartment sodium concentration), w = 0.775 (water volume fraction), S_1 = aTSC and S_2 = aISC. Abbreviations: α2 = pseudo-extracellular volume fraction; aISC = apparent intracellular sodium concentration; aTSC = apparent total sodium concentration; C_1 = pseudo-intracellular sodium concentration

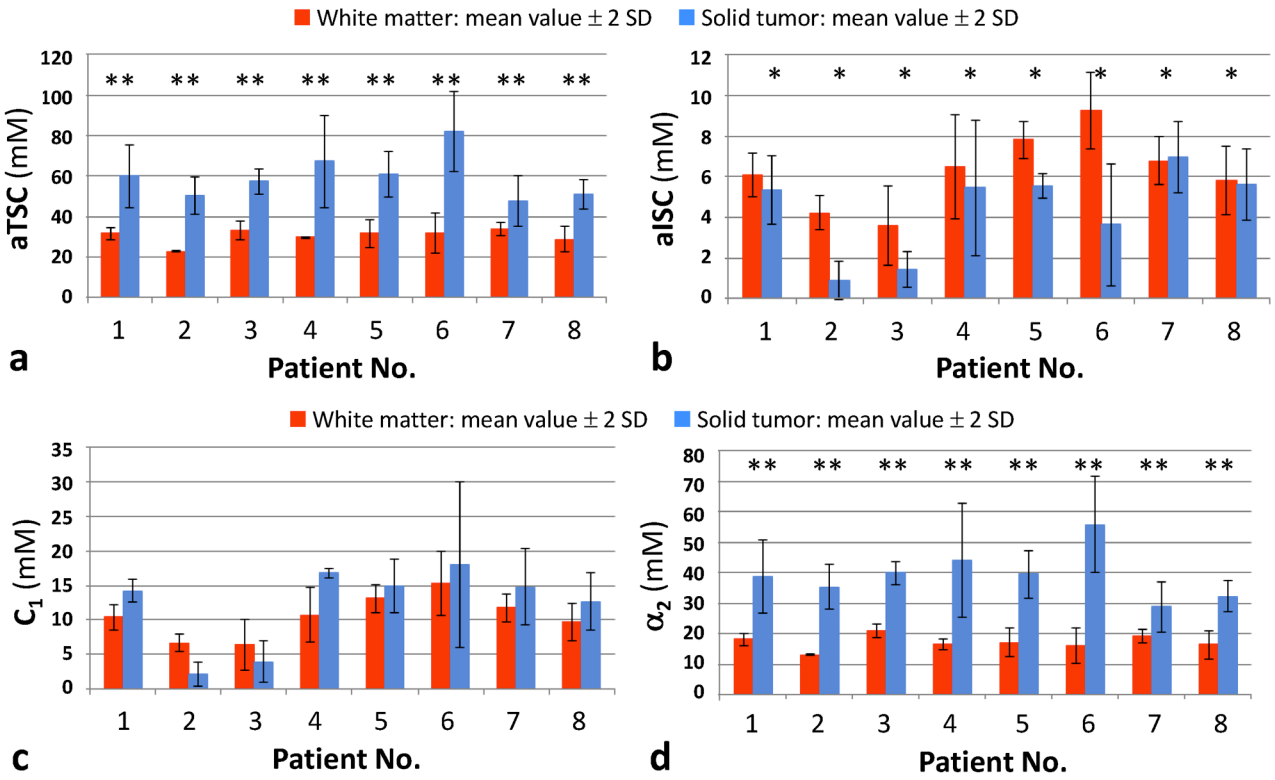

Fig. 2.

Comparison of mean values ± 2 standard deviations (S.D.) of aTSC (A), aISC (B), C_1 (C), and α_2 (D) between normal appearing white matter and solid tumor in each patient. * = statistically significant difference ($p<0.05$); ** = statistically significant difference ($p<0.001$). Abbreviations: α_2 = pseudo-extracellular volume fraction; aISC = apparent intracellular sodium concentration; aTSC = apparent total sodium concentration; C_1 = pseudo-intracellular sodium concentration

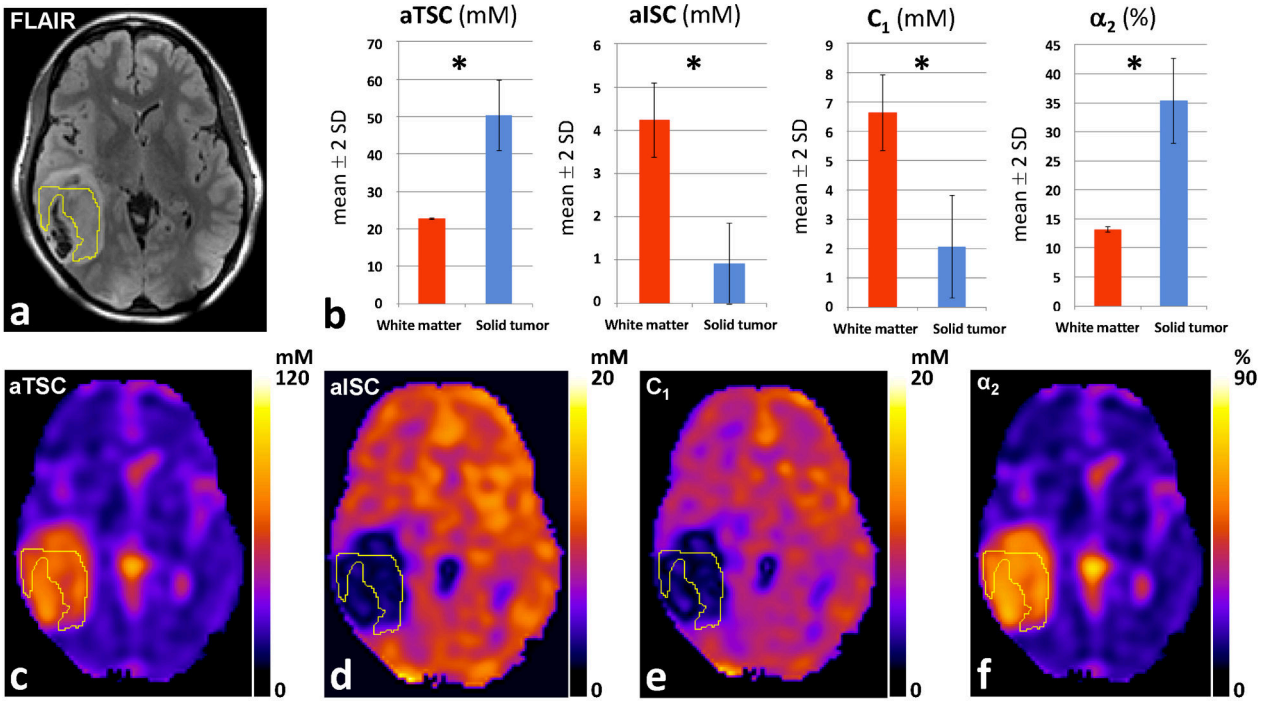

Fig. 3.

Diffuse Astrocytoma, WHO grade II, IDH-mutated. (**A**) Tumor located in the right temporal lobe, with solid portion demonstrating high FLAIR signal on ^{1}H-MRI. (**B**) ^{23}Na-MRI demonstrates in the solid tumor increased values of aTSC and α_2, and decreased values of aISC and C_1 compared to NAWM. (**C**) aTSC map. (**D**) aISC map. (**E**) C_1 map. (**F**) α_2 map. * = statistically significant difference ($p<0.001$). Abbreviations: α_2 = pseudo-extracellular volume fraction; aISC = apparent intracellular sodium concentration; aTSC = apparent total sodium concentration; C_1 = pseudo-intracellular sodium concentration. NAWM = normal appearing white matter

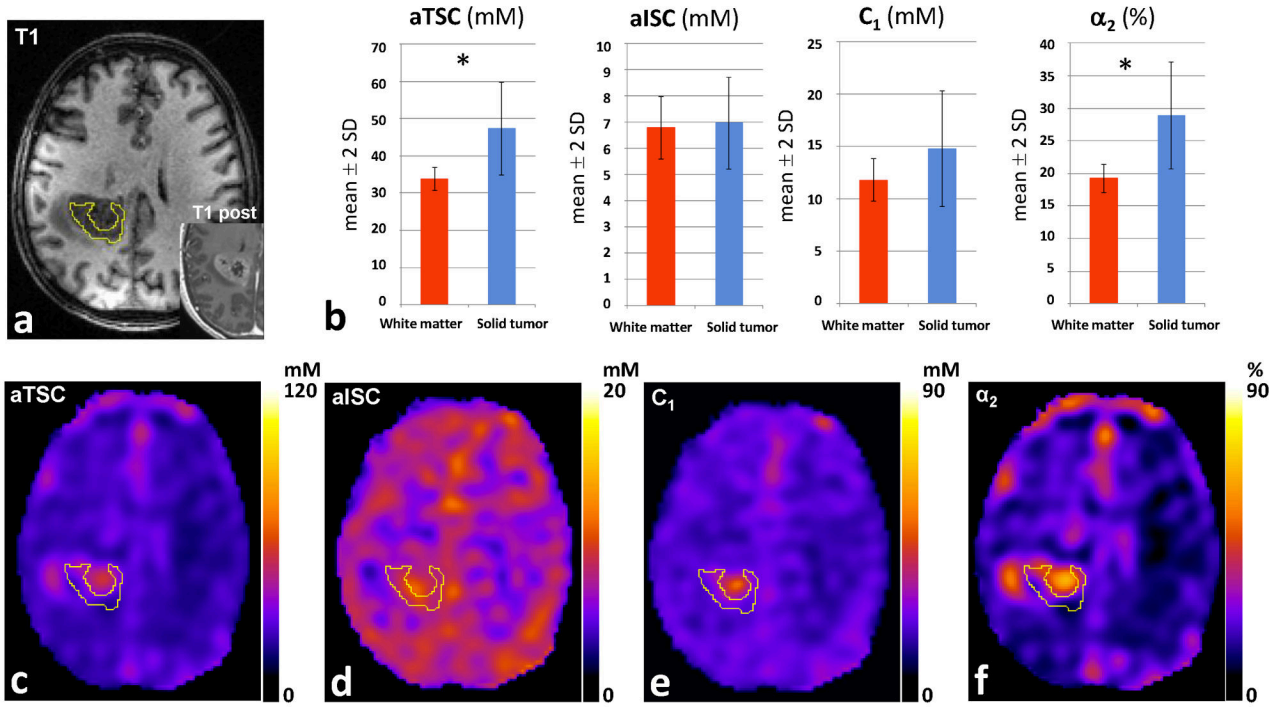

Fig. 4.

Glioblastoma, WHO grade IV, IDH-wildtype. (**A**) Tumor demonstrating heterogeneous contrast enhancement on T1 post-contrast image on ^{1}H-MRI. (**B**) ^{23}Na-MRI demonstrates in the solid tumor increased values of aTSC and α_2 compared to NAWM, while values of aISC and C_1 are similar to NAWM. (**C**) aTSC map. (**D**) aISC map. (**E**) C_1 map. (**F**) α_2 map. * = statistically significant difference ($p<0.05$). Abbreviations: α_2 = pseudo-extracellular volume fraction; aISC = apparent intracellular sodium concentration; aTSC = apparent total sodium concentration; C_1 = pseudo-intracellular sodium concentration. NAWM = normal appearing white matter

Table 1:

Diagnosis, location, and quantitative ^{23}Na measurements (mean and standard deviation) in the normal appearing white mater and solid components of tumor for each patient.

Patient No.	Diagnosis	Location	White matter aTSC	White matter α_2	White matter C_1	White matter aISC	Solid tumor aTSC	Solid tumor α_2	Solid tumor C_1	Solid tumor aISC	Solid tumor aISC / NAWM aISC
1	Oligodendroglioma, grade II, IDH-mutated, 1p/19q-codeleted	Left operculum, cortical and subcortical	31.54 +/− 1.56	18.17 +/− 1.05	10.39 +/− 0.95	6.10 +/− 0.55	59.88 +/− 7.69	38.94 +/− 6.03	14.21 +/− 0.85	5.36 +/− 0.85	0.88
2	Astrocytoma, grade II, IDH-mutated	Right temporal lobe with transmantle extension	22.66 +/− 0.12	13.16 +/− 0.22	6.64 +/− 0.65	4.23 +/− 0.43	50.32 +/− 4.71	35.30 +/− 3.66	2.06 +/− 0.87	0.90 +/− 0.47	0.21
3	Pleomorphic xanthoastrocytoma, grade III	Right centrum semiovale	32.86 +/− 2.35	20.93 +/− 1.05	6.39 +/− 1.87	3.56 +/− 0.98	57.29 +/− 3.15	39.90 +/− 1.94	3.96 +/− 1.53	1.43 +/− 0.45	0.40
4	Probable low grade glioma	Right mesial temporal lobe, cortical and subcortical	29.51 +/− 0.19	16.44 +/− 0.91	10.74 +/− 1.95	6.50 +/− 1.28	67.16 +/− 11.43	44.08 +/− 9.37	16.78 +/− 0.31	5.45 +/− 1.68	0.84
5	Oligodendroglioma, grade II, IDH-mutated, 1p/19q-codeleted	Right frontal lobe, cortical and subcortical	31.72 +/− 3.47	17.07 +/− 2.38	13.11 +/− 1.02	7.82 +/− 0.45	60.81 +/− 5.57	39.49 +/− 3.87	14.97 +/− 1.96	5.53 +/− 0.31	0.71
6	Probable low grade glioma	Right frontal lobe with transmantle extension	31.85 +/− 4.92	16.13 +/− 2.84	15.31 +/− 2.29	9.26 +/− 0.94	81.87 +/− 9.95	55.89 +/− 7.94	18.02 +/− 5.98	3.63 +/− 1.5	0.39
7	Glioblastoma, grade IV, IDH-wildtype	Right centrum semiovale and corpus callosum	33.73 +/− 1.55	19.24 +/− 1.09	11.79 +/− 1.01	6.79 +/− 0.60	47.38 +/− 6.24	28.87 +/− 4.11	14.78 +/− 2.76	6.96 +/− 0.87	1.03
8	Oligodendroglioma, grade II, IDH-mutated, 1p/19q-codeleted	Left frontal lobe, cortical and subcortical	28.65 +/− 3.18	16.30 +/− 2.39	9.63 +/− 1.36	5.83 +/− 0.84	50.80 +/− 3.71	32.26 +/− 2.62	12.68 +/− 2.10	5.63 +/− 0.87	0.97

Note: $\alpha 2$ = extracellular volume fraction; aISC = apparent intracellular sodium concentration; aTSC = apparent total sodium concentration; C_1 = pseudo-intracellular sodium concentration; NAWM = normal appearing white mater.